the Pt_2X systems gives rise to different ground-state structures for Pt_2Cl and Pt_2Br.

Pt_2Br is a moderate semiconductor, with conductivity 10^6 times greater than that of Reihlen's green, $[Pt^{II}(etn)_4][Pt^{IV}(etn)_4Br_2]Br_4 \cdot 4H_2O$ (etn = ethylamine),[50] but 10^6 times weaker than that of $K_2[Pt(CN)_4]Br_{0.3} \cdot 3.2H_2O$. The conductivity shows an unusual temperature dependence and, most likely, it also shows sample dependence, given the sample dependence observed in the Raman data and in the visual appearance. The present conductivity results are consistent with a thermally activated electrical conductivity process also referred to as a hopping process.[42] The actual mechanism may be related to the intrinsic structure as well as to the local states (polarons, bipolarons, kinks) that can arise from chemical defects. Recent resonance Raman studies of $[Pt(en)_2][Pt(en)_2X_2](ClO_4)_4$, where X = Cl or Br, have shown evidence for fine structure in the ν_1(Pt-Br) band, demonstrating the presence of more than one structural species. Conradson et al.[54] attribute this fine structure, in part, to the presence of local states that arise from chemical defects. Baeriswyl and Bishop[55] have recently developed a theory of charge-transfer instability in quasi-1-dimensional mixed-valence metal systems and have calculated optical properties for local states in these solids.

We note that an analogous system that uses iodide ion as the bridging unit between metal dimers, $Pt_2(CH_3CS_2)_4I$, forms a structure at 300 K with translational symmetry that is virtually $(AAB)_n$.[29,30] The conductivity of this material is comparable to those of the Pt_2X systems described here.

Conclusion

This paper presents a study of the translational symmetry properties of a unique class of 1-dimensional materials based on a metal dimer as the synthetic unit. The parent metal dimer complex, $[Pt_2(P_2O_5H_2)_4]^{4-}$, with K^+ as the counterion, provides the basic structural framework.

The translational symmetry, $(AAB)_n$, which we anticipated for Pt_2Br, was not found in any structure, although the observed structure is only slightly different from this translational symmetry. Consideration of the cavity size between Pt_2 units indicates that bromide is more appropriate than chloride for creating a highly symmetric 1-dimensional material with $(AAB)_n$ symmetry. Chloride, which is not as well suited for the K^+/Pt_2 framework as bromide, leads to the $(AABCCB)_n$ structure. The Pt_2Cl and Pt_2Br complexes provide an interesting example of how competing interactions in a quasi 1-dimensional system lead to different ground-state structures. An understanding of the relationship between the structures of these materials, the nature of the local states, and the macroscopic properties such as conductivity is essential in developing materials with useful properties.

Acknowledgment. We thank Dr. Sten Samson for many enlightening discussions regarding structural transformations and Dr. Richard E. Marsh for help in interpreting the X-ray results. This research was supported by National Science Foundation Grants CHE84-19828 (H.B.G.) and CHE82-19039 (X-ray diffraction equipment), the Exxon Educational Foundation (W.P.S.), and the LANL Center for Material Sciences (B.I.S.).

Registry No. $K_4[Pt_2(P_2O_5H_2)_4Cl] \cdot 3H_2O$, 99632-89-0; $K_4[Pt_2(P_2O_5H_2)_4Br] \cdot 3H_2O$, 85553-24-8; $K_4[Pt_2(P_2O_5H_2)_4I]$, 85553-25-9; Pt, 7440-06-4.

Supplementary Material Available: Tables of anisotropic thermal parameters (3 pages); listings of observed and calculated structure factors (27 pages). Ordering information is given on any current masthead page.

(54) Conradson, S. D.; Dallinger, R. F.; Swanson, B. I.; Clark, R. J. H.; Croud, V. B. *Chem. Phys. Lett.* **1987**, *135*, 463.
(55) Baeriswyl, D.; Bishop, A., to be submitted for publication.

Kinetics, Mechanism, and Thermodynamic Aspects of the Interconversion of Complexes of Planar and Nonplanar Metallo-Amido-*N* Groups

Terrence J. Collins*[1a] and John T. Keech[1b]

Contribution No. 7453 from The Chemical Laboratories, California Institute of Technology, Pasadena, California 91125. *Received December 23, 1986*

Abstract: The isomerization kinetics of *trans*- (**1**) and *cis*-α-Os(η^4-CHBA-DCB)$(OPPh_3)_2$ (**2**) (H_4CHBA-DCB = 1,2-bis(3,5-dichloro-2-hydroxybenzamido)-4,5-dichlorobenzene) have been studied for the processes $\mathbf{2} \rightarrow \mathbf{1}$ and $\mathbf{2}^+ \rightleftharpoons \mathbf{1}^+$. The trans isomer contains planar amido-*N* ligands and the cis-α isomer contains nonplanar amido-*N* ligands. Each isomerization is first order in metal complex and zero order in $OPPh_3$. The following mechanisms have been considered: D_L, dissociation of a monodentate ligand followed by isomerization and recoordination; D_{C^-}, dissociation of a phenolate anion followed by isomerization and recoordination; $D_{C\cdot}$, dissociation of a phenoxide radical followed by isomerization and recoordination; T, an intramolecular twist mechanism. In both systems the accumulated evidence is most consistent with T mechanisms. The forward rate constants for the $\mathbf{2} \rightarrow \mathbf{1}$ isomerization and the composite rate constants for the $\mathbf{2}^+ \rightleftharpoons \mathbf{1}^+$ equilibrium show minimal sensitivity to solvent polarity and added *p*-toluenesulfonic acid. Isomerizations conducted in the presence of OP(*p*-tolyl)$_3$ show no evidence of incorporation of OP(*p*-tolyl)$_3$ in the final product. When the $\mathbf{2} \rightarrow \mathbf{1}$ isomerization is conducted in neat 2-mercaptoethanol or in the presence of excess hydroquinone, no evidence of radical intermediates is observed. Variable-temperature studies of the equilibrium $\mathbf{2}^+ \rightleftharpoons \mathbf{1}^+$ yielded ΔH° = 12 (3) kcal·mol^{-1} and ΔS° = 42 (2) eu from a van't Hoff plot. Combining these data with the composite rate constants ($k_{obsd} = k_1 + k_{-1}$) allowed separation of the forward (k_1) and reverse (k_{-1}) rate constants. Activation parameters were evaluated from Eyring plots: for $\mathbf{2}^+ \rightarrow \mathbf{1}^+$, $\Delta H^\ddagger$ = 23.7 (6) kcal·mol^{-1} and $\Delta S^\ddagger$ = 17 (2) eu; for $\mathbf{1}^+ \rightarrow \mathbf{2}^+$, $\Delta H^\ddagger$ = 11.5 (6) kcal·mol^{-1} and $\Delta S^\ddagger$ = −25 (2) eu; for $\mathbf{2} \rightarrow \mathbf{1}$, $\Delta H^\ddagger$ = 21.6 (2) kcal·mol^{-1} and $\Delta S^\ddagger$ = 0.3 (6) eu. The activation parameters are discussed.

The organic amide is a central functional group. Planarity of the organic amide is a structural generality having many notable consequences including, together with hydrogen bonding, a controlling function over the secondary structure of proteins. Organic

0002-7863/88/1510-1162$01.50/0

and theoretical chemists have long appreciated the significance of identifying and understanding the instances of nonplanar amides and of evaluating the activation parameters associated with distorting amides from planarity.[2] Nonplanar amides can exhibit markedly different chemical and physical properties from their planar analogues. Over the last 3 years, we have identified the first cases of distinctly nonplanar organic amide ligands. There are now three separate classes of amido-*N* complexes having large twist angles about the C–N bond: (1) complexes that are thermodynamically stable because of the presence of nonplanar amido-*N* ligands,[2,3] (2) complexes where structural constraints of the coordination sphere necessitate the formation of nonplanar amido-*N* ligands,[3,4] and (3) a complex in which formation of a nonplanar amido-*N* ligand is induced by steric effects.[5] In this report we discuss the first mechanistic study of facile isomerizations of diastereomeric complexes, e.g. **1** and **2**, in which planar and nonplanar amido-*N* ligands are interconverted.

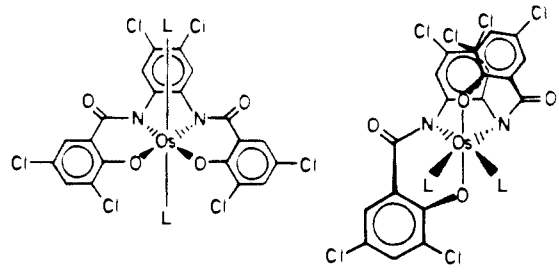

trans 1 cis-α 2

$Os(\eta^4\text{-CHBA-DCB})L_2$

L = $OPPh_3$

Experimental Section

Materials. Acetonitrile (Mallinckrodt) and dichloromethane (Baker) were distilled from calcium hydride prior to use. Benzene (thiophene free; Aldrich) was washed twice with concentrated H_2SO_4 and then distilled. Bromoethane (98%; Aldrich), hydrogen peroxide (30%; Baker), hydroquinone (M.C.B.), magnesium sulfate (Baker), methanol (Baker), nitrosonium tetrafluoroborate (Aldrich), nitrosonium hexafluorophosphate (Pfalz and Bauer), potassium sulfate (MCB) sulfuric acid (concentrated; Baker), *p*-toluenesulfonic acid (98%; MCB), and triphenylphosphine (Strem) were used as received. 2-Mercaptoethanol (98%; MCB) was vacuum distilled prior to use. Ferrocene (98%; Aldrich) was sublimed prior to use. A 0.3 M solution of tri-*p*-tolylphosphine oxide in dichloromethane was prepared by reacting a dichloromethane solution of the parent phosphine with aqueous H_2O_2 (30%) for 30 min, washing once with saturated aqueous K_2SO_3 and three times with distilled water, and drying over $MgSO_4$. Molarity was estimated by ^1H NMR spectroscopy. Tetrabutylammonium perchlorate (Southwestern Analytical Chemicals) was dried, recrystallized twice from acetone/ether, and then dried in vacuo. Silica gel used in column chromatography was 60–200 mesh (Davidson).

Physical Measurements. ^1H NMR spectra were recorded at 89.83 MHz on a JEOL FX-90Q or at 399.78 MHz on a JEOL GX-400. ^{31}P NMR spectra were recorded at 36.28 MHz on a JEOL FX-90Q. Unless otherwise noted, errors were propagated according to

$$\sigma_F^2 = \left[\sum_{i=1}^{n}\left(\frac{\delta F}{\delta x_i}\right)^2 \sigma_{x_i}^2\right]^{1/2}$$

where $F = F(x_1, x_2, ..., x_n)$.[6] Errors of ±5 mV were estimated for E_f measurements.

Syntheses. All reactions were carried out in air unless otherwise noted. The syntheses of *trans*-Os(η^4-CHBA–DCB)$(OPPh_3)_2$ (**1**)[3] and *cis*-α-Os(η^4-CHBA–DCB)$(OPPh_3)_2$ (**2**)[3] have been reported previously.

***trans*-[Os(η^4-CHBA–DCB)$(OPPh_3)_2$]BF_4 (1^+).** *trans*-Os(η^4-CHBA–DCB)$(OPPh_3)_2$ (11.8 mg, 9.09 μmol) and excess nitrosonium tetrafluoroborate were added to a round-bottom flask (25 mL), which was subsequently sealed with a rubber septrum and cooled (−78 °C). Cold dichloromethane (−78 °C, 10 mL) was added by syringe, and the mixture was kept cold for 2 h, during which the insoluble nitrosonium salt reacted with the complex to afford a 0.91 mM turquoise solution, which was used for the kinetic studies. The synthesis and characterization of *trans*-[Os(η^4-CHBA–DCB)$(OPPh_3)_2$]PF_6 have been described in a previous report.[3]

Equilibrium Measurements. Cyclic voltammetry and controlled-potential electrolyses were performed with a Princeton Applied Research Model 173/179 potentiostat/digital coulometer equipped with positive-feedback *iR* compensation and a Model 175 universal programmer. Current–voltage curves were recorded on a Houston Instruments Model 2000 X-Y recorder. Cyclic voltammetric experiments were conducted in standard two-compartment cells. Linear plots of peak current vs the square root of scan rate over the range 20–500 $mV \cdot s^{-1}$ were measured for all reversible couples. Controlled-potential electrolysis was used to oxidize **1** to an equilibrium mixture of 1^+ and 2^+. Compound **1** (12.4 mg, 9.55 μmol) was added to a three-compartment vacuum-line electrochemical cell. Working and counter electrodes were platinum gauze. A silver wire was used as a quasi-reference electrode. After the loaded cell was dried in vacuo for 12 h, sufficient dichloromethane was vacuum-transferred into the cell to form a 1 mM solution of **1**. Bulk electrolysis by 1 faraday/mol of osmium cleanly generated a mixture of 1^+ and 2^+.

Normal-pulse voltammetry,[7] used to measured K^+ for the equilibrium between the 1^+ and 2^+ diastereomers, was performed on a Bioanalytical Systems, Inc., BAS-100 electrochemical analyzer with a 0.03-cm^{-2} platinum-disk working electrode. A 50-ms pulse width, a pulse period of 1 s, and a scan rate of 20 $mV \cdot s^{-1}$ were used. The equilibrium constant was taken to be equal to the ratio of wave heights from the two monocation/osmium(IV) reductions. The temperature of the cell was regulated by immersion in the reservoir of a Neslab Endocal RTE-4 refrigerated circulating bath filled with aqueous ethylene glycol (35% w/w). The recorded cell temperature was the reservoir temperature, which was monitored with a thermometer calibrated at 0 °C in a distilled water ice bath. After the reservoir temperature was changed, 20 min was allowed for the cell to come to thermal equilibrium before the measurements were taken. Equilibrium constants were measured between −2.2 and +30 °C.

Kinetic Rate Measurements. Kinetic rates for the $2 \rightarrow 1$ isomerization and the approach to the $2^+ \rightleftharpoons 1^+$ equilibrium were measured by UV–vis spectroscopy in various solvent systems and at different temperatures. UV–vis spectra were recorded on a Hewlett-Packard HP8450A spectrophotometer equipped with an HP89100A temperature controller and an HP89101A temperature control unit. Solvent (3.0–3.5 mL) was added to a glass cuvette, which was sealed with a rubber septum and brought to thermal equilibrium. The appropriate amount of an osmium reagent was added to the cuvette, and the automatic data collection was started. Kinetics were consistently found to be first-order in osmium reagent. For all systems studied stable time-independent A_∞ or A_e values were obtained in most runs. Occasionally, a very small amount of reduction to the osmium(IV) state was found at the end of a run for the $2^+ \rightleftharpoons 1^+$ study; for this reason data were analyzed by the Kedzy–Swinbourne (K–S) method.[8a] Although the K–S method is typically applied to first-order kinetics, a similar expression can be derived for the rate of approach to first-order equilibria. The observed rate, however, is actually the sum of the forward and reverse rates. Given the equilibrium

$$A \underset{k_{-1}}{\overset{k_1}{\rightleftharpoons}} B$$

the expression for absorbance at time t is as follows

$$A_t = (A_0 - A_e)e^{-(k_1+k_{-1})t} + A_e$$

where A_e is the equilibrium absorbance.[8b] At time $t + \Delta$

$$A_{t+\Delta} = (A_0 - A_e)e^{-(k_1+k_{-1})(t+\Delta)} + A_e$$

From these two equations the following relation can be derived:

(1) (a) Dreyfus Teacher-Scholar, 1986–1990; Alfred P. Sloan Research Fellow, 1986–1988. Present address: Department of Chemistry, Carnegie Mellon University, 4400 Fifth Street, Pittsburgh, PA 15213. (b) Present address: Eastman Kodak Co., Photographic Research Laboratories, Rochester, NY 14650.

(2) Collins, T. J.; Coots, R. J.; Furutani, T. T.; Keech, J. T.; Peake, G. T.; Santarsiero, B. D. *J. Am. Chem. Soc.* **1986**, *108*, 5333–5339, and references therein.

(3) Anson, F. C.; Collins, T. J.; Gipson, S. L.; Keech, J. T.; Krafft, T. E.; Peake, G. T. *J. Am. Chem. Soc.* **1986**, *108*, 6593–6605.

(4) (a) Anson, F. C.; Christie, J. A.; Collins, T. J.; Coots, R. J.; Furutani, T. T.; Gipson, S. L.; Keech, J. T.; Krafft, T. E.; Santarsiero, B. D.; Spies, G. H. *J. Am. Chem. Soc.* **1984**, *106*, 4460–4472. (b) Barner, C. J.; Collins, T. J.; Mapes, B. E.; Santarsiero, B. D. *Inorg. Chem.* **1986**, *25*, 4322–4333.

(5) Collins, T. J.; Lai, T.; Peake, G. T. *Inorg. Chem.* **1987**, *26*, 1674–1677.

(6) Peters, D. G.; Hayes, J. M. *Chemical Separations and Measurements*; Saunders: Philadelphia, 1974; pp 6–37.

(7) Bard, A. J., Faulkner, L. F., Eds. *Electrochemical Methods. Fundamentals and Applications*; Wiley: New York, 1980; pp 106–199.

(8) (a) Moore, J. W.; Pearson, R. G. *Kinetics and Mechanism*, 3rd ed.; Wiley: New York, 1981; p 72. (b) *Ibid.*, p 304.

$$A_t = e^{(k_1+k_{-1})\Delta}A_{t+\Delta} + A_e(1 - e^{(k_1+k_{-1})\Delta})$$

Thus, when $A_{t+\Delta}$ is plotted against A_t, the slope equals $\exp[(k_1 + k_{-1})/\Delta]$ and the A_e equals [(y intercept)/(slope)].

In all K–S analyses, rates were calculated by using Δ time increments of greater than 1 half-life. If a rate had a large standard deviation, then the calculated A_∞ or A_e values from the K–S analysis were used to plot ln ($A_\infty - A_t$) vs t. Rates determined from these secondary analyses generally had smaller relative errors than those from the initial K–S analyses. Extinction coefficients (ϵ) for all compounds at the wavelengths at which rates were calculated are listed in Table I.

Rate Measurements of the Approach to Equilibrium of *cis*-α-$2^+ \rightleftharpoons$ *trans*-1^+. An aliquot from a 0.91 mM stock solution of 1^+ (0.2–0.3 mL) was transferred with a cold syringe into the cuvette containing cooled solvent. Four isosbestic points were observed at wavelengths of 369, 422, 442, and 638 nm. Data were collected between 300 and 800 nm. Observed rate constants ($k_{obsd} = k_1 + k_{-1}$) were calculated from the 344-, 544-, and 744-nm data and then averaged. The rates had first-order dependence on the concentration of osmium. Forward and reverse rate constants were separated by combining the data with the equilibrium constants ($K^+ = k_1/k_{-1}$). Activation parameters were determined for the forward and reverse processes from the separated rates at temperatures of 0–20 °C in CH_2Cl_2. Observed rates were also determined at 0 °C in 1.0 mM to 0.5 M $OPPh_3$ in CH_2Cl_2, 100 mM TBAP in CH_2Cl_2 and CH_3CN, and 100 mM p-toluenesulfonic acid in CH_3CN. The observed rates are summarized in Table II. Equilibrium constants at various temperatures are contained in Table III. Separate forward and reverse rate constants are summarized in Table IV.

Rate Measurements of the cis-α → trans Isomerization, $2 \rightarrow 1$. Material that contained both cis-α and trans complexes (3:1 by ^1H NMR) was used for kinetic rate determinations (1.5–2.0 mg/experiment). Data were collected between 402 and 800 nm. Two isosbestic points were observed at 422- and 629-nm wavelengths. Rate constants were calculated from the 462-, 566-, and 694-nm data and then averaged. The rates had first-order dependence on the concentration of **2**. Activation parameters were determined from the rate measurements at temperatures of between 5 and 35 °C in CH_2Cl_2. Rates were also calculated at 35 °C in 1.0 mM to 2.0 M $OPPh_3$ in CH_2Cl_2, 100 mM TBAP in CH_2Cl_2, CH_3CN, and C_6H_6, 100 mM p-toluenesulfonic acid in CH_3CN, 100 mM hydroquinone in CH_3CN, and neat 2-mercaptoethanol. The rate data are summarized in Table V.

Examination for Possible OP(p-Tol)$_3$ Exchange for $OPPh_3$ in 1. *trans*-Os[η^4-CHBA–DCB)$(OPPh_3)_2$ (**1**) (10 mg, 7.7 μmol) was added to a CH_2Cl_2 solution of OP(p-Tol)$_3$ (p-Tol = p-tolyl; 2.6 mL, 100 equiv), and the mixture was stirred (3.5 h). All osmium products were precipitated by the addition of methanol and were examined by ^1H NMR and ^{31}P NMR spectroscopies. No signals other than those expected for **3** were observed.

Examination for Possible OP(p-Tol)$_3$ Exchange for $OPPh_3$ in $1^+ \rightleftharpoons 2^+$ Equilibrium. A 25-mL round-bottom flask was charged with **1** (26 mg, 20 μmol) and excess nitrosonium hexafluorophosphate and was sealed with a rubber septum. After the flask was cooled (−78 °C), cold CH_2Cl_2 (−78 °C, 210 mL) was added, and the mixture reacted to form pure 1^+ within 2 h. The solution was transferred to a cold flask to remove the excess nitrosonium hexafluorophosphate, and the OP(p-Tol)$_3$ solution was added (6.7 mL, 100 equiv). The solution was warmed to room temperature to initiate isomerization and was allowed to stand for 2 min (10 half-lives based on composite rate constant). Ferrocene (18 mg, 5 equiv) was added as a CH_2Cl_2 solution to reduce the osmium to a neutral mixture of **1** and **2**. The **2** present was allowed to isomerize to **1** (3.5 h) at room temperature. All osmium products were precipitated by the addition of methanol, passed down a short silica gel column with excess CH_2Cl_2, and recrystallized from CH_2Cl_2/CH_3OH. The column material retained none of the highly colored osmium complexes. The product was examined by ^1H NMR spectroscopy. A number of minute signals were observed in the aliphatic region. If the largest of the signals is that of bound OP(p-Tol)$_3$, then the upper limit for OP(p-Tol)$_3$ incorporation is 0.5% by integration. The cumulative upper limit, if all minute signals in the aliphatic region are attributed to OP(p-Tol)$_3$, is 3%.

Results and Discussion

Four isomerization mechanisms that might account for the cis-$\alpha \rightleftharpoons$ trans isomerizations are shown in Scheme I. These mechanisms have been considered before in isomerization and racemization processes of octahedral chelate complexes.[9-11] The

(9) (a) Serpone, N.; Bickley, D. G. In *Progress in Inorganic Chemistry; Inorganic Reaction Mechanisms*; Edwards, J. O., Ed.; Interscience: New York, 1972; Vol. 17, Part II, pp 391–566. (b) The $\Delta \rightarrow \Lambda$ isomerization of $[Co(oxalate)_3]^{3-}$ takes place by anionic oxalate dissociation, D_{C^-}, and is acid catalyzed. *Ibid.*, pp 416–424.

Table I. Extinction Coefficients for Compounds Studied at Points of Maximum Δ(Absorbance) between the Cis-α and Trans Diastereomers (ϵ, L·mol^{-1}·cm^{-1})

compound	λ, nm	ϵ(cis-α)	ϵ(trans)
$[Os(\eta^4$-CHBA–DCB$)(OPPh_3)_2]^+$	344	7.6×10^3	9.0×10^3
	544	7.0×10^3	4.1×10^3
	744	1.1×10^3	2.6×10^3
$Os(\eta^4$-CHBA–DCB$)(OPPh_3)_2$	462	2.6×10^3	1.8×10^3
	566	2.0×10^3	1.5×10^3
	694	7.0×10^2	1.1×10^3

Table II. Measured Composite Rate Constants for Cis-$\alpha \rightleftharpoons$ Trans Equilibrium of $[Os(\eta^4$-CHBA–DCB$)(OPPh_3)_2]^+$ [a]

T, °C	anion	solvent	k_{obsd},[a] s^{-1}
0	BF_4	CH_2Cl_2	$1.86\ (1) \times 10^{-2}$
5	BF_4	CH_2Cl_2	$2.75\ (2) \times 10^{-2}$
10	BF_4	CH_2Cl_2	$5.01\ (4) \times 10^{-2}$
15	BF_4	CH_2Cl_2	$8.33\ (5) \times 10^{-2}$
20	BF_4	CH_2Cl_2	$1.26\ (1) \times 10^{-1}$
0	PF_6	CH_2Cl_2	$1.87\ (1) \times 10^{-2}$
0	BF_4	1 mM $OPPh_3/CH_2Cl_2$	$1.85\ (1) \times 10^{-2}$
0	BF_4	10 mM $OPPh_3/CH_2Cl_2$	$1.92\ (1) \times 10^{-2}$
0	BF_4	50 mM $OPPh_3/CH_2Cl_2$	$1.90\ (1) \times 10^{-2}$
0	BF_4	100 mM $OPPh_3/CH_2Cl_2$	$1.85\ (1) \times 10^{-2}$
0	BF_4	500 mM $OPPh_3/CH_2Cl_2$	$2.10\ (4) \times 10^{-2}$
0	BF_4	100 mM TBAP/CH_2Cl_2	$1.98\ (2) \times 10^{-2}$
0	PF_6	CH_3CN	$1.36\ (3) \times 10^{-3}$
0	PF_6	100 mM $CH_3C_6H_4SO_3H/CH_3CN$	$1.92\ (2) \times 10^{-2}$

[a] Values in parentheses are standard deviations in the last digit.

Table III. Measured Equilibrium Constants for Cis-$\alpha \rightleftharpoons$ Trans Equilibrium of $[Os(\eta^4$-CHBA–DCB$)(OPPh_3)_2]^+$ [a]

T, °C	K([trans]/[cis-α])[a]	T, °C	K([trans]/[cis-α])[a]
30.2	1.74	16.6	0.615
25.9	1.38	12.0	0.438
21.3	1.06	7.5	0.345
21.2	1.05	2.0	0.269
21.0	0.919	−2.2	0.140

[a] Measured by normal-pulse voltammetry with 100 mM TBAP/CH_2Cl_2 as solvent. Errors in measurement estimated at ±10%.

Table IV. Derived Forward (k_1) and Reverse (k_{-1}) Rate Constants for Cis-$\alpha \rightleftharpoons$ Trans Equilibrium of $[Os(\eta^4$-CHBA–DCB$)(OPPh_3)_2]^+$ [a]

T, °C	k_1,[a] s^{-1}	k_{-1},[a] s^{-1}
0	$2.96\ (2) \times 10^{-3}$	$1.57\ (10) \times 10^{-2}$
5	$6.06\ (3) \times 10^{-3}$	$2.14\ (10) \times 10^{-2}$
10	$1.47\ (5) \times 10^{-2}$	$3.54\ (12) \times 10^{-2}$
15	$3.16\ (10) \times 10^{-2}$	$5.16\ (16) \times 10^{-2}$
20	$5.91\ (24) \times 10^{-2}$	$6.7\ (3) \times 10^{-2}$

[a] Values in parentheses are standard deviations in the last digits.

Scheme I. Possible Isomerization Mechanisms

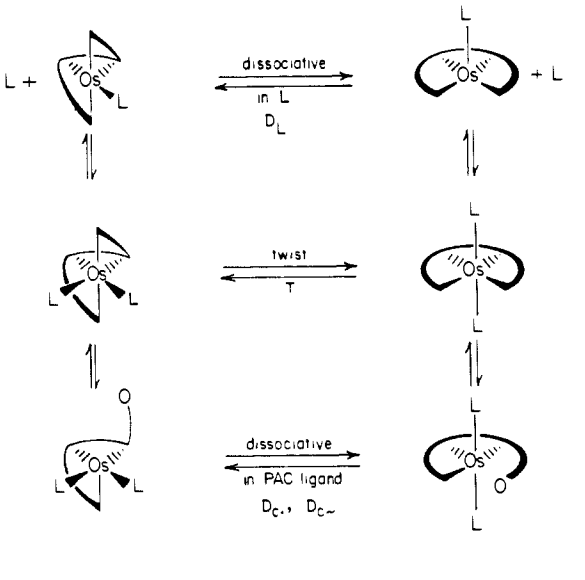

Table V. Measured Rate Contants for Cis-α → Trans Isomerization of Os(η^4-CHBA-DCB)($OPPh_3$)$_2$[a]

T, °C	solvent	k_{obsd}, s^{-1}
5	CH_2Cl_2	7.38 (5) × 10^{-5}
10	CH_2Cl_2	1.54 (1) × 10^{-4}
15	CH_2Cl_2	2.84 (1) × 10^{-4}
20	CH_2Cl_2	5.56 (2) × 10^{-4}
25	CH_2Cl_2	1.07 (2) × 10^{-3}
30	CH_2Cl_2	2.01 (1) × 10^{-3}
35	CH_2Cl_2	3.72 (2) × 10^{-3}
35	1 mM $OPPh_3/CH_2Cl_2$	3.60 (1) × 10^{-3}
35	10 mM $OPPh_3/CH_2Cl_2$	3.61 (1) × 10^{-3}
35	50 mM $OPPh_3/CH_2Cl_2$	3.54 (1) × 10^{-3}
35	100 mM $OPPh_3/CH_2Cl_2$	3.37 (1) × 10^{-3}
35	500 mM $OPPh_3/CH_2Cl_2$	3.19 (4) × 10^{-3}
35	1.0 M $OPPh_3/CH_2Cl_2$	2.90 (2) × 10^{-3}
35	1.5 M $OPPh_3/CH_2Cl_2$	3.03 (1) × 10^{-3}
35	2.0 M $OPPh_3/CH_2Cl_2$	2.45 (3) × 10^{-3}
35	100 mM TBAP/CH_2Cl_2	7.19 (19) × 10^{-3}
35	CH_3CN	2.98 (3) × 10^{-3}
35	100 mM $CH_3C_6H_4SO_3H/CH_3CN$	1.98 (19) × 10^{-3}
35	C_6H_6	6.31 (12) × 10^{-3}
35	100 mM p-$C_6H_4(OH)_2/CH_3CN$	2.62 (5) × 10^{-3}
35	$HSCH_2CH_2OH$	1.86 (4) × 10^{-3}

[a] Values in parentheses are standard deviations in the last digit(s).

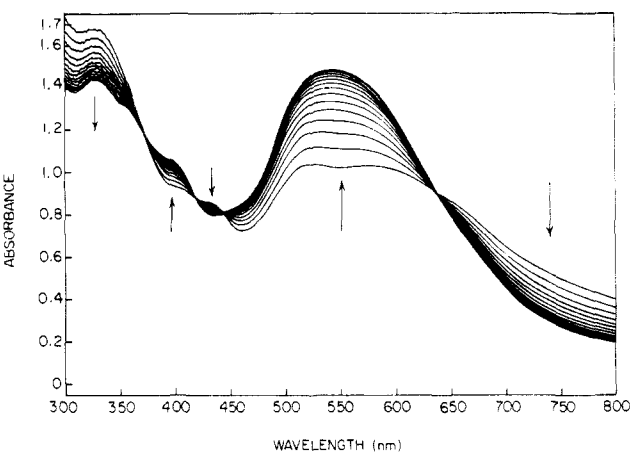

Figure 1. UV-vis spectral monitoring of 2^+ → 1^+ approach to equilibrium in dichloromethane at 0 °C.

simplest invokes a concerted intramolecular "twist" (T mechanism). The D_L, D_C., and D_C- mechanisms involve bond breaking and formation. A system was found to be suitable for mechanistic studies at two oxidation states. Oxidation of *trans*-Os(η^4-CHBA-DCB)($OPPh_3$)$_2$ (**1**) by either chemical or electrochemical methods produces both the trans and cis-α cationic complexes, $\mathbf{1}^+$ and $\mathbf{2}^+$, respectively. Pure isomers can be isolated at low temperatures and isomerize to an equilibrium mixture upon warming. Following reduction of the low-temperature mixture with ferrocene, the neutral cis-α complex, **2**, can be isolated by chromatography. When **2** is warmed in solution, it rapidly converts to the thermodynamically stable trans diastereomer **1**. The isomerization can be conveniently followed by UV-vis spectroscopy (Figure 1). The mechanisms of (1) the cationic $\mathbf{1}^+ \rightleftharpoons \mathbf{2}^+$ equilibrium and (2) the neutral **2** → **1** isomerization have been probed.

Mechanistic Probes. The D_L mechanism can be probed by addition of high concentrations of free ligand L, which can decrease the observed rate by reducing the concentration of the five-coordinate intermediate in favor of the starting material. However, lack of observed rate suppression does not necessarily rule out a D_L process. The rate laws for the T and D_L mechanisms are shown in Figure 2. The observed rate constant, k_{obsd}, for the T mechanism equals the isomerization rate constant, k_1, whereas

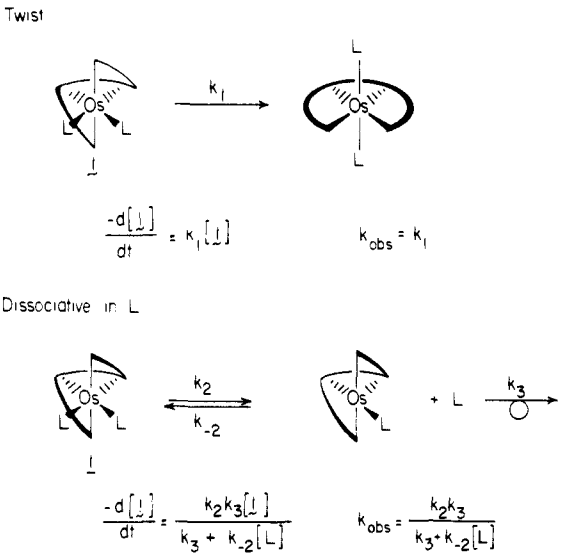

Figure 2. Rate laws for T and D_L mechanisms.

that of the D_L mechanism has the complex expression shown. If $k_3 >> k_{-2}[L]$, no rate suppression should be observed with increasing concentrations of L. A further test for the D_L mechanism is positive incorporation of a labeled (or closely related) ligand, L', into the isomerized product. The zwitterionic intermediate of a D_C- process might have different stability as solvent polarity and ionic strength are altered. Rates were measured in the following solvents (in order of increasing polarity): benzene (ϵ(25 °C) = 2.3[12a]) < dichloromethane (ϵ(25 °C) = 8.9[12b]) < acetonitrile (ϵ(25 °C) = 36.2[12b]). Experiments were also run both in 100 mM *p*-toluenesulfonic acid in acetonitrile and in neat acetonitrile to probe for interactions between the proton and a possible phenoxide anion.[9b] Finally, 100 mM TBAP solutions in dichloromethane were used to probe rate changes as a function of ionic strength. Hydrogen atom sources were used as radical traps for a possible phenoxide radical intermediate (e,g., 2-mercaptoethanol[13] and hydroquinone). Reactions between trapping reagents and the osmium complexes would be expected to generate products other than the isomerized species.

Activation parameters and estimated bond strengths have been used to distinguish the D_L, D_C-, and D_C. mechanisms. The rates of reactions proposed to proceed through T mechanisms are usually solvent-independent.[14a-c] Many of the ΔS^* values are surprising. Ray et al. found large negative entropy factors (−41.5 and −55.3 eu) for the rates of optical inversion of tris(biguanide)cobalt(III) and tris(phenylbiguanide)cobalt(III).[11] Similarly, strikingly negative entropy factors of between −119 and −177 eu have been reported by Bond et al. from electrochemically measured rate constants for the cis → trans isomerization of $[M(CO)_2(DPM)_2]^+$

(10) Bailar, J. C., Jr. *J. Inorg. Nucl. Chem.* **1958**, *8*, 165–175.
(11) (a) Ray, P.; Dutt, N. K. *J. Indian Chem. Soc.* **1943**, *20*, 81–92. (b) *Ibid.* **1941**, *18*, 289–297.

(12) Weast, R. C., Ed. *Handbook of Chemistry and Physics*; CRC: Cleveland, OH, 1975; E55–E56. (b) Gordon, A. J.; Ford, R. A. *The Chemists Companion*; Wiley: New York, 1972; p 5.
(13) 2-Mercaptoethanol is a common reducing agent used to cleave disulfide bonds between cysteine residues.[13a] Thiols can also react as electron-transfer reagents.[13b] Reactions of thiols and $Mn(acac)_3$, for instance, produce $Mn(acac)_2$, acetylacetone, and 0.5 equiv of disulfide.[13c] Similar reactions occur between thiols and $Fe(octanoate)_3$, producing $Fe(octanoate)_2$, octH, and 0.5 equiv of disulfide.[13d] The standard reduction potential for 2-mercaptoethanol is pH dependent and is −0.54 V (vs SCE) at pH 11.5 in water,[13e] sufficient strength to reduce $\mathbf{1}^+$ and $\mathbf{2}^+$. This restricted the use of 2-mercaptoethanol to the isomerization of **2** → **1**. (a) Stryer, L. *Biochemistry*, 2nd ed.; Freeman: San Francisco, 1981; pp 32–36. (b) Cullis, C. F.; Trimm, D. L. *J. Chem. Soc., Faraday Trans. 1* **1968**, *46*, 144–149. (c) Nakaya, T.; Arabori, H.; Imoto, M. *Bull. Chem. Soc. Jpn.* **1970**, *43*, 1888–1889. (d) Wallace, T. J. *J. Org. Chem.* **1966**, *31*, 3071–3074. (e) Meites, L.; Zuman, P. *Electrochemical Data*; Wiley: New York, 1974; Vol. A, Part 1, p 30.
(14) (a) Bond, A. M.; Grabaric, B. S.; Grabaric, Z. Z. *Inorg. Chem.* **1978**, *17*, 1013–1019. (b) *Ibid.* 2153–2157. (c) Bond, A. M.; Colton, R.; McDonald, M. E. *Ibid.* 2842–2847. (d) Bond, A. M.; Carr, S. W.; Colton, R. *Organometallics* **1984**, *3*, 541–548. (e) Darensbourg, D. J. *Inorg. Chem.* **1979**, *18*, 14–17. (f) Connor, K. A.; Walton, R. A. *Organometallics* **1983**, *2*, 169–171. (g) Datta, S.; Dezube, B.; Kouba, J. K.; Wreford, S. S. *J. Am. Chem. Soc.* **1978**, *100*, 4404–4412.

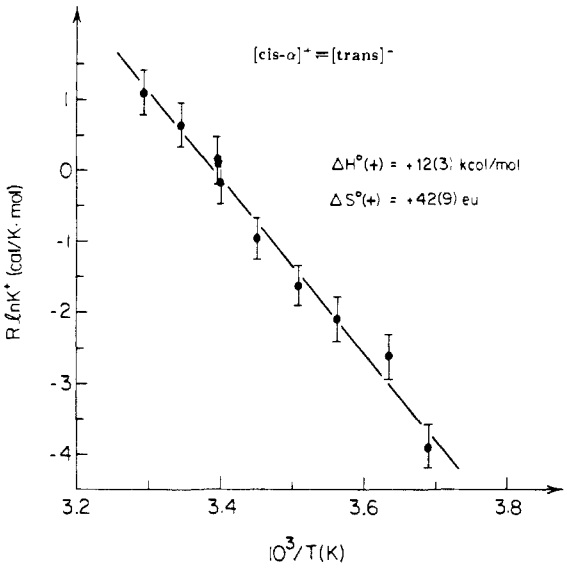

Figure 3. van't Hoff plot for the $2^+ \rightleftharpoons 1^+$ equilibrium.

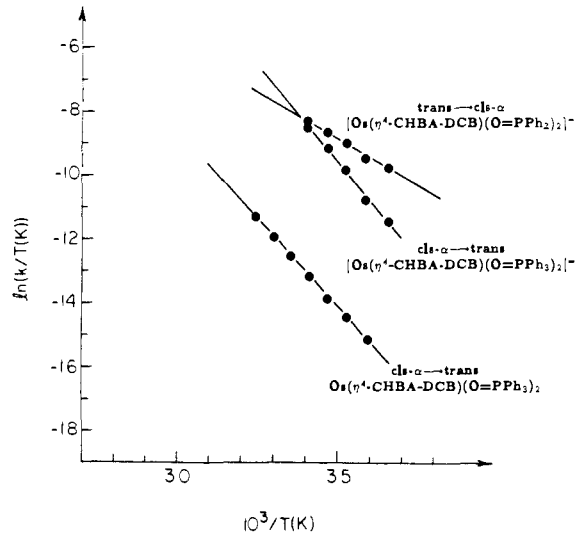

Figure 4. Eyring plots for the isomerization reactions.

and $[M(CO)_2(DEM)_2]^+$ (M = Cr, Mo, and W; DMP = bis(diphenylphosphino)methane; DEM = bis(diethylphosphino)methane).[14a-d] Such entropy factors seem unusual for processes involving no association in the transition state. Entropy factors between −9.8 and −0.44 eu have been measured for other isomerizations proposed to proceed through T mechanisms.[14e,g]

Thermodynamic Studies of the $2^+ \rightleftharpoons 1^+$ Equilibrium. At room temperature the oxidation of **1** produces an equilibrium mixture of 1^+ and 2^+. At −78 °C 1^+ is the only oxidation product. Nitrosonium salts are useful oxidants at low temperature in dichloromethane, excess being removed by filtration when the oxidation is complete.

In a previous report,[3] a thermodynamic ladder was derived for the cis-$\alpha \rightleftharpoons$ trans equilibrium of Os(η^4-CHBA-DCB)(*t*-Bupy)$_2$ at the monocationic, neutral Os(IV), monoanionic Os(III), and dianionic Os(II) oxidation states. This was accomplished by measuring the cis-$\alpha \rightleftharpoons$ trans equilibrium constant at the monocation stage, K^+, by normal-pulse voltammetry (NPV) and combining this value with the formal potentials of the osmium electrochemical couples for both isomers to derive the isomerization equilibrium constants at the other three oxidation states. These data were used, together with spectroscopic and structural studies, to show that the isomerization processes are driven by increased ligand → metal bonding for the nonplanar amido-*N* ligands of the cis-α isomers relative to the planar amido-*N* ligands of the trans isomers. A similar study is reported here for the bis(phosphine oxide) complexes; measurements of K^+ at different temperatures made it possible to calculate the reaction enthalpy, $\Delta H°$, and entropy, $\Delta S°$, from a van't Hoff plot.

A sample of **1** was electrooxidized by 1 faraday/mol of osmium to the cationic state. The ratio of the concentration of each isomer, or K^+ for cis-$\alpha \rightleftharpoons$ trans equilibrium, was determined by NPV. Equilibrium constants range between 1.74 at 30.2 °C and 0.14 at −2.2 °C (Table II). The van't Hoff plot of these data (Figure 3) is linear (r = −0.986). The calculated reaction enthalpy ($\Delta H°$) is 12 (3) kcal·mol^{-1} and the entropy ($\Delta S°$) is 42 (2) eu. The $\Delta H°$ value indicates that there is stronger overall bonding in the cis-α isomer, consistent with our previous results that increased bonding occurs in the nonplanar amido-*N* complexes (such as *cis*-α-2^+) relative to the analogous planar amido-*N* complexes (such as *trans*-1^+).[3] The large positive $\Delta S°$ term may result from ion-pairing or solvation differences for the two species, with greater association for the cis-α diastereomer. Unfortunately, the propogated uncertainties of the $\Delta H°$ and $\Delta S°$ values were too large to provide reliable estimates for the equilibria at the osmium(IV) and osmium(III) states.

Kinetic Studies of the $2^+ \rightleftharpoons 1^+$ Isomerizations. The rate law for the conversion of 1^+ to an equilibrium mixture of 1^+ and 2^+ was first-order in osmium concentration. Because this isomerization reaction is reversible, the observed rate constant, k_{obsd}, equals the sum of the forward and reverse rate constants, $k_1 + k_{-1}$, for the equilibrium $2^+ \rightleftharpoons 1^+$. The composite rate constants were measured in different media and are summarized in Table II.

Table VI. Isomerization Activation Parameters

process	k,[a] s^{-1}	ΔH^*, kcal·mol^{-1}	ΔS^*, eu
$2 \rightarrow 1$	7.34 (3) × 10^{-4}	21.6 (2)	0.3 (6)
$2^+ \rightarrow 1^+$	8.17 (3) × 10^{-2}	23.7 (6)	17 (2)
$1^+ \rightarrow 2^+$	8.06 (4) × 10^{-2}	11.5 (6)	−25 (2)

[a] Rate constant at 22 °C.

Comparisons of composite rate constants under different conditions must be treated with caution. The forward and reverse rates need not respond identically to changes in conditions. The composite rate constants for the $2^+ \rightleftharpoons 1^+$ isomerizations show little sensitivity to changes in conditions. The composite rate constants for the isomerizations of the BF_4^- and PF_6^- salts of 1^+ are identical, which suggests that both salts have about the same degree of charge separation in dichloromethane. The rate constants in dichloromethane are virtually independent of the concentration of $OPPh_3$ up to 500 mM. When the isomerization equilibrium was established in the presence of OP(*p*-Tol)$_3$ (100 equiv), there was no evidence for incorporation in the equilibrated product as determined by ^{1}H NMR after reduction to the osmium(IV) state. The composite rate constant measured in 100 mM TBAP in dichloromethane is unchanged from that in the pure solvent. When more polar acetonitrile is employed as solvent, the rate decreases by a factor of 13.7 relative to dichloromethane. The composite rate is increased in acetonitrile in the presence of 100 mM *p*-toluenesulfonic acid by a factor of 14. Thus, changes in polarity both increase and decrease the composite rates by relatively small factors, probably pointing away from a D_C mechanism in total. 2-Mercaptoethanol and hydroquinone could not be used to probe for the $D_{C'}$ mechanism because both reagents reduce 2^+ and 1^+. The $D_{C'}$ reaction pathway would pass through a 13-electron, five-coordinate, cationic intermediate; considerable sensitivity of the observed rate constants to the solvent polarity would be expected for this mechanism. In sum, the relative insensitivity of the composite rate constants to the nature of the medium suggests the T mechanism is the most consistent choice.

Separate activation parameters for the forward and reverse rates have been calculated from the composite rate constants ($k_{obsd} = k_1 + k_{-1}$) and the K^+ equilibrium constants ($K^+ = k_1/k_{-1}$) at temperatures between 0 and 20 °C. The derived forward and reverse rate constants are summarized in Table IV. Eyring plots of this data are shown in Figure 4. Activation parameters derived from these plots are summarized in Table VI.

Isomerization of $2 \rightarrow 1$. Calculated rate constants for the isomerization of *cis*-α-Os(η^4-CHBA-DCB)($OPPh_3$)$_2$ under various

conditions are listed in Table V. When measured in dichloromethane at 35 °C, the rates show no systematic decrease with increasing concentrations of up to 2.0 M $OPPh_3$, a $OPPh_3$ to Os ratio of 6000:1. The UV–vis spectra are not perturbed by the excess $OPPh_3$. No incorporation of $OP(p\text{-Tol})_3$ was observed by ^1H and ^{31}P NMR when the isomerization was carried out in a large excess of this potential ligand. These experiments suggest that the D_L mechanism can be discounted. Activation parameters were calculated from the rate constants in dichloromethane at temperatures of 5–35 °C. An Eyring plot of these data is shown in Figure 4. Calculated activation parameters are contained in Table VI.

The **2** → **1** isomerization rate increases slightly as the polarity decreases, $k(HSCH_2CH_2OH) < k(CH_3CN) < k(CH_2Cl_2) < k(C_6H_6)$, suggesting that the D_C- mechanism is not operative. In 2-mercaptoethanol, the expected isomerization product, **1**, is obtained. Thus, if a diradical intermediate is formed via a D_C. mechanism, isomerization and recoordination are both faster than reaction with the thiol solvent ([thiol] ≈ 14.3 M, conservative lower limit for detection ≈5%).

Summary

The insensitivity of the systems studied to changes in the solvent polarity and the presence of acid suggest that the D_C- mechanism is unlikely at both oxidation states. The similarity and the rather low $\Delta H^{\ddagger}$ values for the $2^+ \rightarrow 1^+$ and **2** → **1** isomerizations in the nonpolar solvent dichloromethane (Table VI) are evidence against a D_C- mechanism where heterolysis is rate determining. The trend in rate constants with changes in solvent polarity do not appear to support the D_C- mechanism. The lack of evidence for monodentate ligand exchange during isomerization suggests that the D_L mechanism is unlikely.[15] Isomerizations performed in the presence of the radical traps 2-mercaptoethanol and hydroquinone did not alter the reaction course, suggesting that the D_C. mechanism is not important at the osmium(IV) state. Rates of reaction between the comparable phenoxide radicals and 2-mercaptoethanol or hydroquinone are not available. It is possible that isomerization of the five-coordinate intermediate and phenoxide radical recapture could be more rapid than reaction with the radical traps. Different mechanisms could be operating at different oxidation states. A D_C. mechanism, in which a phenolate ligand is oxidized to a phenoxide radical, is conceivable at the monocationic state. A T mechanism is arguably more likely at this state than at the Os(IV) oxidation state because there is one less nonbonding $d\pi$ electron on the metal center. Fewer $d\pi$ electrons in the cationic complexes might result in decreased repulsions between the $d\pi$ electrons and those of the anionic ligand sites, stabilizing the transition state in the T mechanism. This might explain the 100-fold greater rate for isomerization of 2^+ compared with **2**. The relative insensitivity of the composite rate constant to the polarities of the solvent media is more consistent with a T than a D_C. mechanism, where a highly unsaturated, cationic intermediate is invoked. The similarity of the $\Delta H^{\ddagger}$ values for the two cis-α → trans isomerizations should be noted (Table VI) and might also be consistent with a T mechanism. However, this similarity might also be considered evidence for a D_C. mechanism with rate-determining bond homolysis. At the present time there is insufficient bond strength data available to judge whether or not the $\Delta H^{\ddagger}$ values represent reasonable numbers for the Os–O bond strengths in these systems.

The accumulated evidence consistently suggests that the T mechanism most reasonably describes the isomerizations of the systems studied. While the focus here has been upon processes occurring at a transition-metal center, the isomerization reactions interconvert cis-α and trans diastereomers where the enthalpy difference is primarily a result of the presence of nonplanar amido-*N* ligands in the former and planar amido-*N* ligands in the latter.

Acknowledgment. We acknowledge the Rohm and Haas Co., the Atlantic Richfield Corp. of America, and the National Science Foundation (Grant CHE-84-06198) for support of this work. J.T.K. thanks the Standard Oil for the award of a Standard Oil Fellowship in Chemical Catalysis, W. R. Grace for the award of a W. R. Grace Fellowship, and Shell for the award of a Shell Doctoral Fellowship.

Registry No. 1^+, 103851-58-7; $1^+BF_4^-$, 111112-46-0; 2^+, 103957-52-4.

(15) It is plausible that extruded phosphine oxide ligand could remain in a cage with the five-coordinate intermediate and be recaptured before any cage decomposition could occur.